

Supporting Information

Compound Defects and Thermoelectric Properties in Ternary CuAgSe-based Materials

Xiaobei Wang,^{a,b,c} Pengfei Qiu,^{a,b} Tiansong Zhang,^b Dudi Ren,^{a,b} Lihua Wu,^{a,b,c} Xun Shi,^{*a,b} Jihui Yang,^{*d} and Lidong Chen^{*a,b,e}

^a*State Key Laboratory of High Performance Ceramics and Superfine Microstructure, Shanghai Institute of Ceramics, Chinese Academy of Sciences, Shanghai 200050, China. E-mail: xshi@mail.sic.ac.cn; cld@mail.sic.ac.cn*

^b*CAS Key Laboratory of Materials for Energy Conversion, Shanghai Institute of Ceramics, Chinese Academy of Sciences, Shanghai 200050, China*

^c*University of Chinese Academy of Sciences, 19 Yuquan Road, Beijing 100049, China*

^d*Materials Science and Engineering Department, University of Washington, Seattle, Washington 98195-2120, USA. E-mail: jihuiy@uw.edu*

^e*Shanghai Institute of Materials Genome, Shanghai 200050, China*

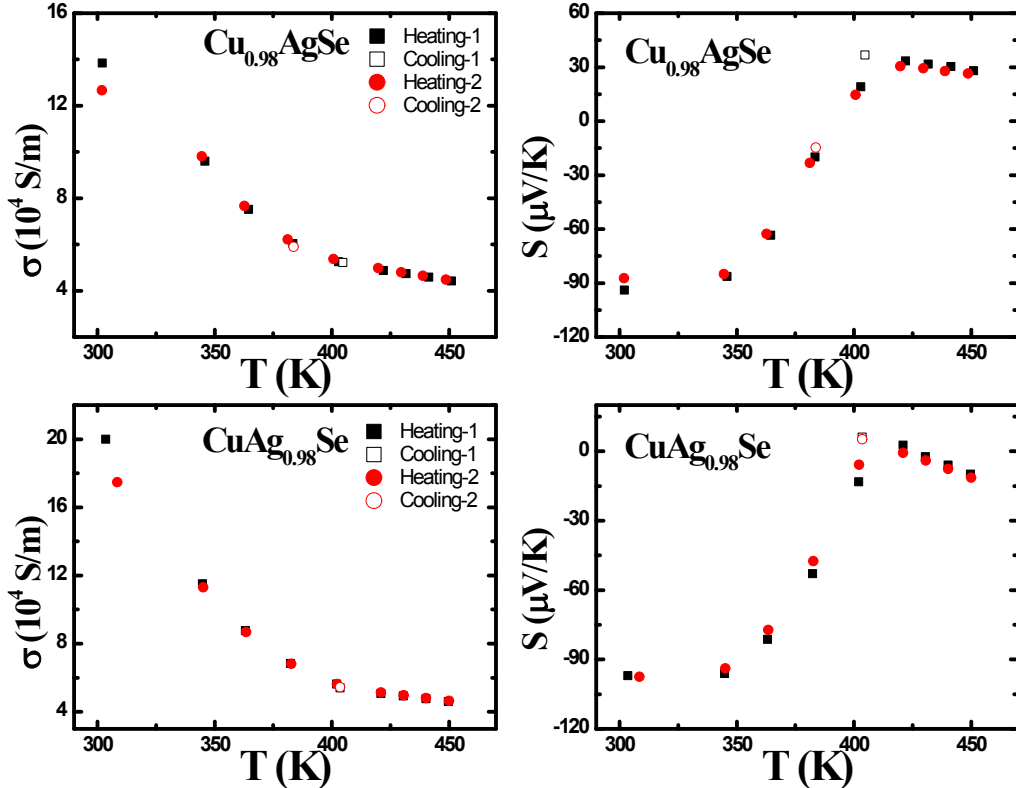


Fig. S1 Cycle measurements of electrical conductivity σ and thermopower S from 300 K to 450 K for sample $\text{Cu}_{0.98}\text{AgSe}$ and $\text{CuAg}_{0.98}\text{Se}$.

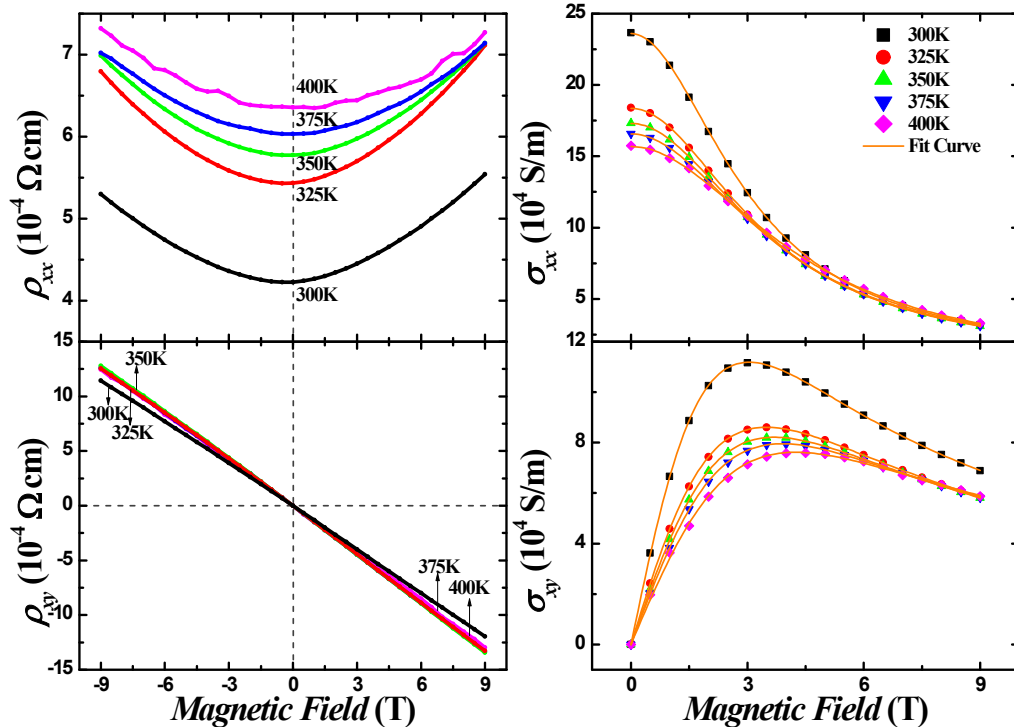


Fig. S2 Magnetic field dependence of longitudinal electrical resistivity ρ_{xx} (a) and Hall resistivity ρ_{xy} (b) of β - CuAgSe from 300 K to 400 K, and the calculated longitudinal conductivity σ_{xx} (c) and Hall conductivity σ_{xy} (d). The solid lines in (c) and (d) are the fits using Equation (3) and (4).

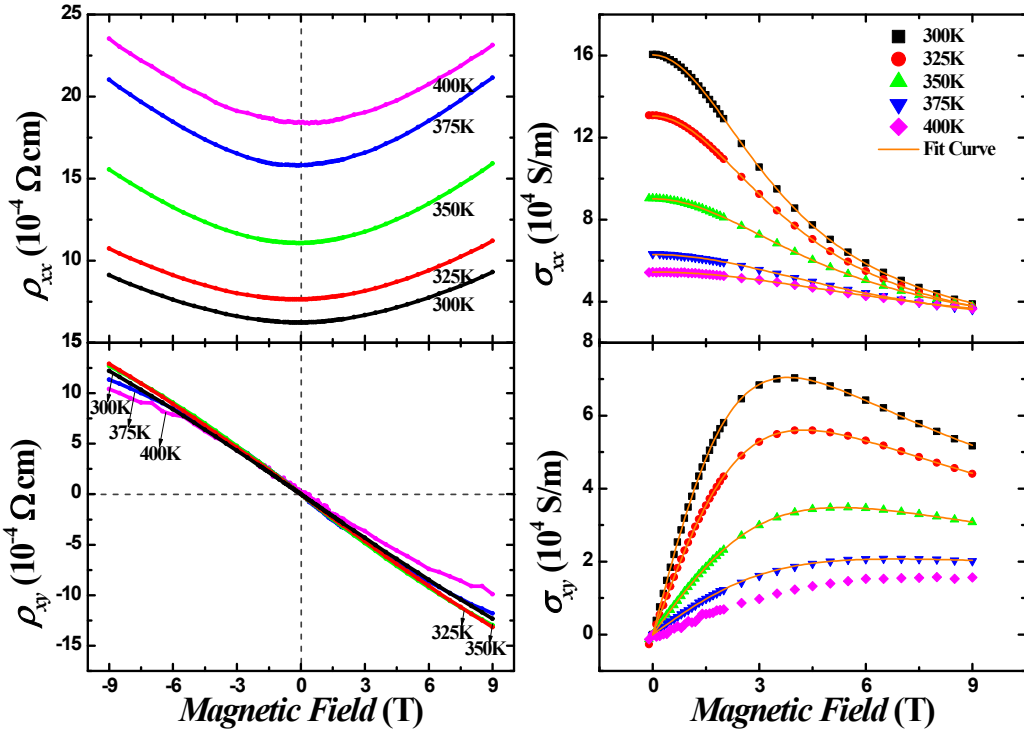


Fig. S3 Magnetic field dependence of longitudinal electrical resistivity ρ_{xx} (a) and Hall resistivity ρ_{xy} (b) of $\text{Cu}_{0.99}\text{AgSe}$ from 300 K to 400 K, and the calculated longitudinal conductivity σ_{xx} (c) and Hall conductivity σ_{xy} (d). The solid lines in (c) and (d) are the fits using Equation (3) and (4).

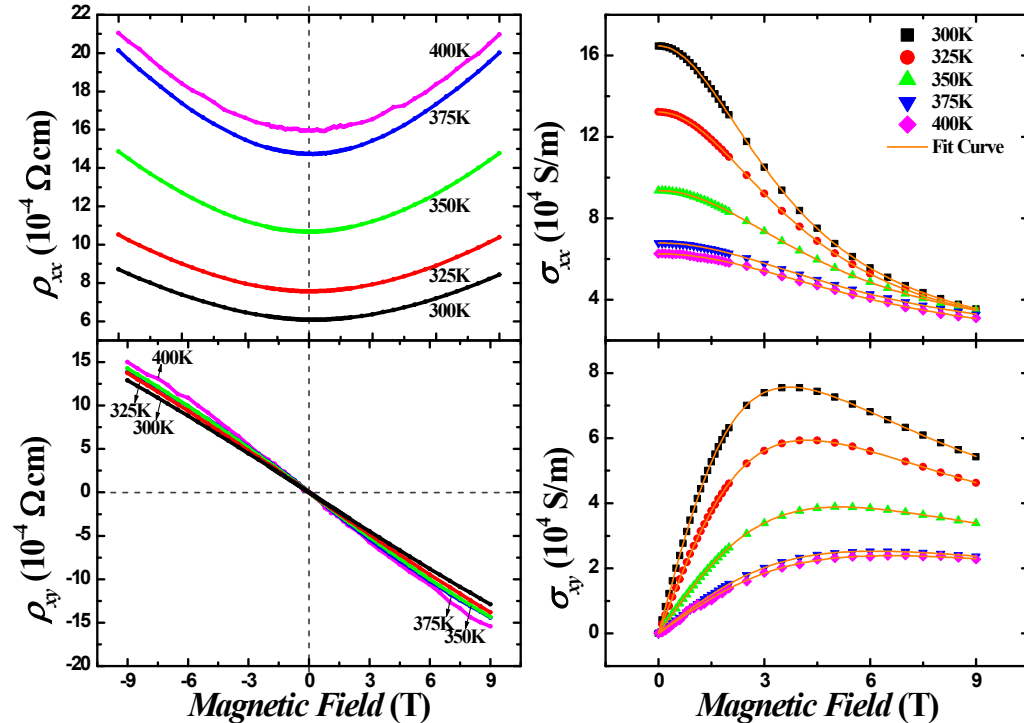


Fig. S4 Magnetic field dependence of longitudinal electrical resistivity ρ_{xx} (a) and Hall resistivity ρ_{xy} (b) of $\text{CuAg}_{0.99}\text{Se}$ from 300 K to 400 K, and the calculated longitudinal conductivity σ_{xx} (c) and Hall conductivity σ_{xy} (d). The solid lines in (c) and (d) are the fits using Equation (3) and (4).

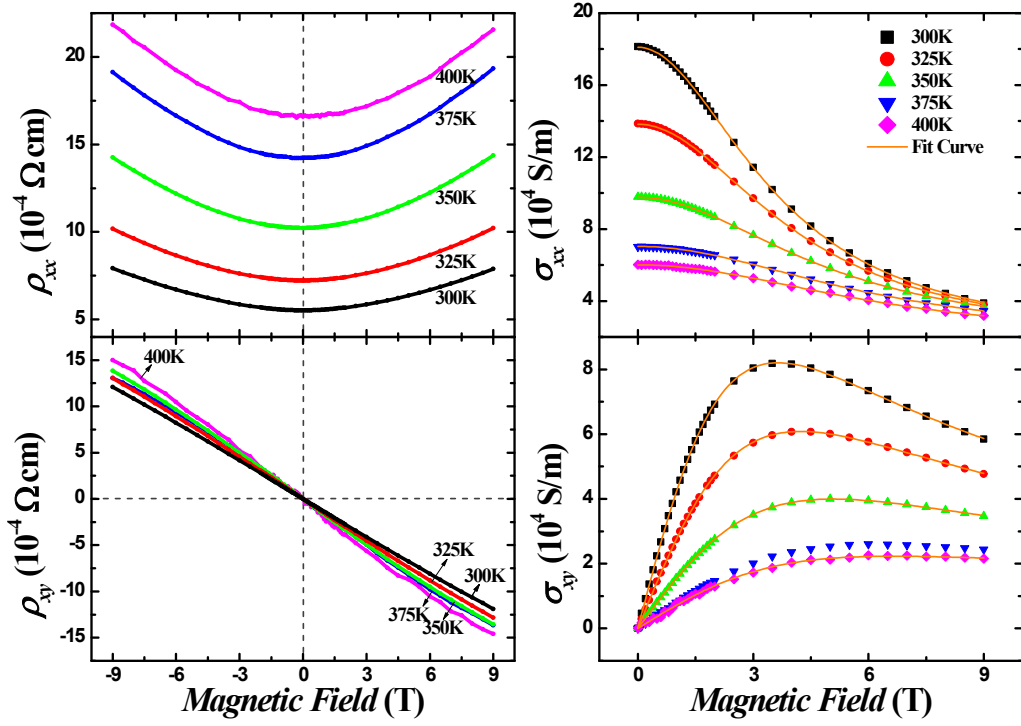


Fig. S5 Magnetic field dependence of longitudinal electrical resistivity ρ_{xx} (a) and Hall resistivity ρ_{xy} (b) of CuAg_{0.98}Se from 300 K to 400 K, and the calculated longitudinal conductivity σ_{xx} (c) and Hall conductivity σ_{xy} (d). The solid lines in (c) and (d) are the fits using Equation (3) and (4).

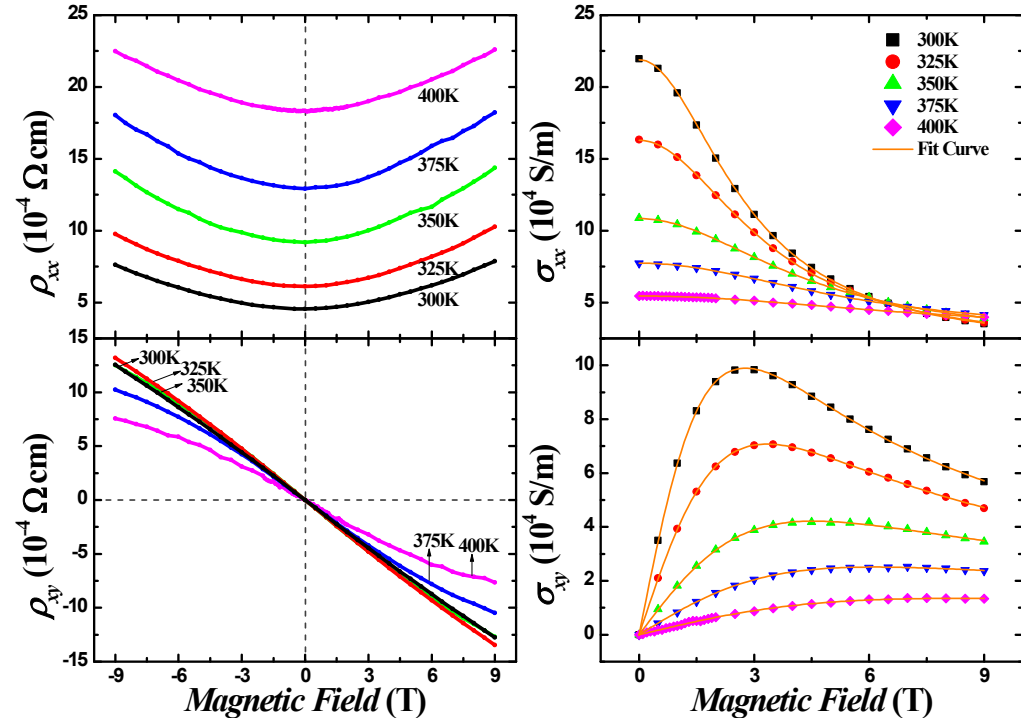


Fig. S6 Magnetic field dependence of longitudinal electrical resistivity ρ_{xx} (a) and Hall resistivity ρ_{xy} (b) of CuAgSe_{1.04} from 300 K to 400 K, and the calculated longitudinal conductivity σ_{xx} (c) and Hall conductivity σ_{xy} (d). The solid lines in (c) and (d) are the fits by using Equation (3) and (4).



Fig. S7 Ingot samples after high temperature annealing. CuAg_{1.01}Se, Cu_{1.01}AgSe, and CuAgSe_{0.99} display the same phenomenon as the left sample with the metallic Ag on the surface. The samples in the Section of 3.1.1-3.1.4 are the right one without obvious metallic Ag observed.

Table S1. Fitting parameters for sample β -CuAgSe.

T(K)	n _{xx} (10 ¹⁸ cm ⁻³)	μ_{xx} (10 ⁴ cm ² /V-s)	C _{xx} ($\Omega^{-1}m^{-1}$)	n _{xy} (10 ¹⁸ cm ⁻³)	μ_{xy} (10 ⁴ cm ² /V-s)	C _{xy} (10 ⁻³)
300	4. 32	0. 33	8914. 24	4. 21	0. 33	2. 57
325	3. 80	0. 29	8811. 22	3. 72	0. 29	2. 25
350	3. 85	0. 27	6830. 86	3. 76	0. 27	1. 80
375	3. 88	0. 26	6057. 52	3. 84	0. 26	1. 94
400	4. 17	0. 23	3654. 34	3. 99	0. 24	2. 31

Table S2. Fitting parameters for sample Cu_{0.99}AgSe.

T(K)	n _{xx} (10 ¹⁸ cm ⁻³)	μ_{xx} (10 ⁴ cm ² /V-s)	C _{xx} ($\Omega^{-1}m^{-1}$)	n _{xy} (10 ¹⁸ cm ⁻³)	μ_{xy} (10 ⁴ cm ² /V-s)	C _{xy} (10 ⁻³)
300	3. 38	0. 26	17837. 22	3. 25	0. 27	7. 84
325	2. 96	0. 24	17564. 74	2. 87	0. 24	9. 18
350	2. 25	0. 19	20613. 82	2. 15	0. 20	15. 83
375	1. 62	0. 16	22539. 92	1. 17	0. 18	87. 57

Table S3. Fitting parameters for sample Cu_{0.98}AgSe.

T(K)	n _{xx} (10 ¹⁸ cm ⁻³)	μ_{xx} (10 ⁴ cm ² /V-s)	C _{xx} ($\Omega^{-1}m^{-1}$)	n _{xy} (10 ¹⁸ cm ⁻³)	μ_{xy} (10 ⁴ cm ² /V-s)	C _{xy} (10 ⁻³)
300	3. 39	0. 24	17126. 60	3. 27	0. 24	5. 93
325	2. 67	0. 20	18887. 09	2. 55	0. 20	6. 28
350	2. 02	0. 17	20636. 09	1. 86	0. 17	4. 92
375	1. 48	0. 14	22236. 39	1. 22	0. 15	21. 14
400	1. 12	0. 12	24620. 52	0. 80	0. 13	62. 87

Table S4. Fitting parameters for sample CuAg_{0.99}Se.

T(K)	n _{xx} (10 ¹⁸ cm ⁻³)	$\mu_{xx}(10^4 \text{ cm}^2/\text{V}\cdot\text{s})$	C _{xx} ($\Omega^{-1}\text{m}^{-1}$)	n _{xy} (10 ¹⁸ cm ⁻³)	$\mu_{xy}(10^4 \text{ cm}^2/\text{V}\cdot\text{s})$	C _{xy} (10 ⁻³)
300	3.51	0.27	13629.32	3.44	0.27	5.29
325	3.10	0.24	13767.59	3.04	0.24	6.52
350	2.46	0.20	16103.31	2.39	0.20	11.16
375	1.91	0.17	17245.32	1.77	0.17	21.99
400	1.97	0.15	14044.87	1.68	0.17	36.66

Table S5. Fitting parameters for sample CuAg_{0.98}Se.

T(K)	n _{xx} (10 ¹⁸ cm ⁻³)	$\mu_{xx}(10^4 \text{ cm}^2/\text{V}\cdot\text{s})$	C _{xx} ($\Omega^{-1}\text{m}^{-1}$)	n _{xy} (10 ¹⁸ cm ⁻³)	$\mu_{xy}(10^4 \text{ cm}^2/\text{V}\cdot\text{s})$	C _{xy} (10 ⁻³)
300	3.75	0.27	16023.47	3.63	0.28	7.35
325	3.20	0.24	16409.91	3.09	0.24	9.71
350	2.47	0.20	18383.47	2.37	0.20	16.60
400	1.78	0.15	16628.66	1.37	0.18	67.87

Table S6. Fitting parameters for sample CuAgSe_{1.04}.

T(K)	n _{xx} (10 ¹⁸ cm ⁻³)	$\mu_{xx}(10^4 \text{ cm}^2/\text{V}\cdot\text{s})$	C _{xx} ($\Omega^{-1}\text{m}^{-1}$)	n _{xy} (10 ¹⁸ cm ⁻³)	$\mu_{xy}(10^4 \text{ cm}^2/\text{V}\cdot\text{s})$	C _{xy} (10 ⁻³)
300	3.50	0.36	17979.08	3.38	0.36	3.44
325	3.02	0.30	18668.98	2.89	0.30	5.10
350	2.37	0.23	22767.92	2.24	0.23	16.11
375	1.83	0.17	26563.32	1.56	0.18	48.51
400	1.25	0.13	28859.85	1.15	0.13	47.33